Nanostructured Sexithiophene/Clay Hybrid Mutilayers: A Comparative Structural and Morphological Characterization

Xiaowu Fan, Jason Locklin, Ji Ho Youk, Wally Blanton, Chuanjun Xia, and Rigoberto Advincula*

Alabama Tri-campus Materials Science Program and Department of Chemistry, University of Alabama at Birmingham, Birmingham, Alabama 35294-1240

Received October 29, 2001. Revised Manuscript Received March 6, 2002

Ultrathin films prepared from inorganic and organic materials are of increasing interest as hybrid nanocomposite materials. We have investigated for the first time the formation of nanostructured ultrathin films of montmorillonite clay (**MONT**) and a bicationic sexithiophene derivative (**6TN**) using the layer-by-layer self-assembly approach. The main goal is to investigate the structure and layer ordering of these films suitable for future applications in organic semiconductor devices. We have compared the structure and morphology of **6TN/MONT** multilayer thin films prepared from pure water and 0.1 M NaCl systems. The **6TN** amphiphile showed unique aggregation behavior both in solution and on the surface, which changes with the presence of salts and a THF cosolvent. On clay surfaces, the **6TN** aggregates deposited from saline solutions have a more uniform size distribution and surface coverage than that from a pure water system. This was verified by UV−vis spectra, X-ray diffraction (XRD), and atomic force microscopy (AFM). The idea of incorporating more **6TN** species absorbed on the surface while yielding a smoother surface morphology have a great significance in semiconductor device fabrication.

Introduction

The structure and properties of polyelectrolyte/clay self-assembled ultrathin films have been intensively and extensively investigated. These well-ordered, nanostructured thin films are easily fabricated using layer-by-layer deposition[1] and have tremendous promise in applications such as optical and electronic materials.[2,3] Furthermore, they are also ideal systems for the study of the various theories in interface science and intercalation thermodynamics of organic species in a confined and tethered environment.[4]

A great deal of work has been done regarding the characterization of these hybrid nanocomposite films. Silicate clay species, such as montmorillonite and hectorite, are negatively charged upon hydration and possess unique layered morphology. Kleinfeld and Ferguson reported the incorporation of these clay sheets into thin films using the electrostatic layer-by-layer approach,[5] which showed moisture-sensitive characteristics suitable for humidity sensing.[6] In-depth structural investigation of film thickness and interlayer spacing of clay particles was accomplished by Kotov and coworkers through a series of surface-sensitive techniques which included surface plasmon spectroscopy (SPS), X-ray reflectivity, and X-ray diffraction (XRD).[7] The gas permeation properties of these films were also investigated. Also of great importance was the determination of the mechanism of the layer-by-layer alternate self-assembly of the clay multilayers.[7,8] Film surface smoothness is of crucial importance for real commercial applications such as packaging and coatings and the use of atomic force microscopy (AFM) and mathematical modeling have provided great insight into the structural development and surface morphology of the multilayer system. The mechanism for the high degree of order of this kind of multilayer has also been suggested.[9,10] Very recently, organic species intercalated into this system has been extended to charged dye molecules.[11] A protonated coumarin dye has been applied to the self-assembly process.

In recent years, sexithiophene derivatives have attracted great attention due to their high charge mobility and on/off ratios as *p*-type organic semiconductors.[12] They have been widely studied as promising candidates for organic field-effect transistors (OFETs) and organic light-emitting diodes (OLEDs).[13,14] One major problem is the poor solubility of most sexithiophene derivatives rendering solution deposition techniques improbable for the fabrication of thin film devices. As a result, the vacuum deposition technique has been the most com-

(1) Fendler J. H. *Chem. Mater.* **1996**, *8*, 1616.
(2) Decher, G. *Science* **1997**, *277*, 1232.
(3) He, J.-A.; Samuelson, L.; Li, L.; Kumar, J.; Tripathy, S. K. *Langmuir* **1998**, *14*, 1674.
(4) Giannelis E. P.; Krishnamoorti, R.; Manias, E. *Adv. Polym. Sci.* **1998**, 38.
(5) Kleinfeld, E. R.; Ferguson, G. S. *Science* **1994**, *265*, 370.
(6) Kleinfeld, E. R.; Ferguson, G. S. *Chem. Mater.* **1995**, *7*, 2327.
(7) Kotov, N. A.; Haraszti, T.; Turi, L.; Zavala, G.; Geer, R. E.; Dekany, I.; Fendler, J. H. *J. Am. Chem. Soc.* **1997**, *119*, 6821.
(8) Kleinfeld, E. R.; Ferguson, G. S. *Chem. Mater.* **1996**, *8*, 1575.
(9) Van Duffel, B.; Schoonheydt, R. A.; Grim, C. P. M.; DeSchryver, F. C. *Langmuir* **1999**, *15*, 7520.
(10) Kotov, N. A.; Magonov, S.; Tropsha, E. *Chem. Mater.* **1998**, *10*, 886.
(11) Kim, D. W.; Blumstein, A.; Kuma, J.; Tripathy, S. K. *Chem. Mater. Commun.* **2001**, *13*, 565.
(12) Müllen, K., Wegner, G., Ed. *Electronic Materials: The Oligomer Approach*; Wiley-VCH: Weinheim, 1998.

10.1021/cm011519c CCC: $22.00
Published on Web 04/18/2002

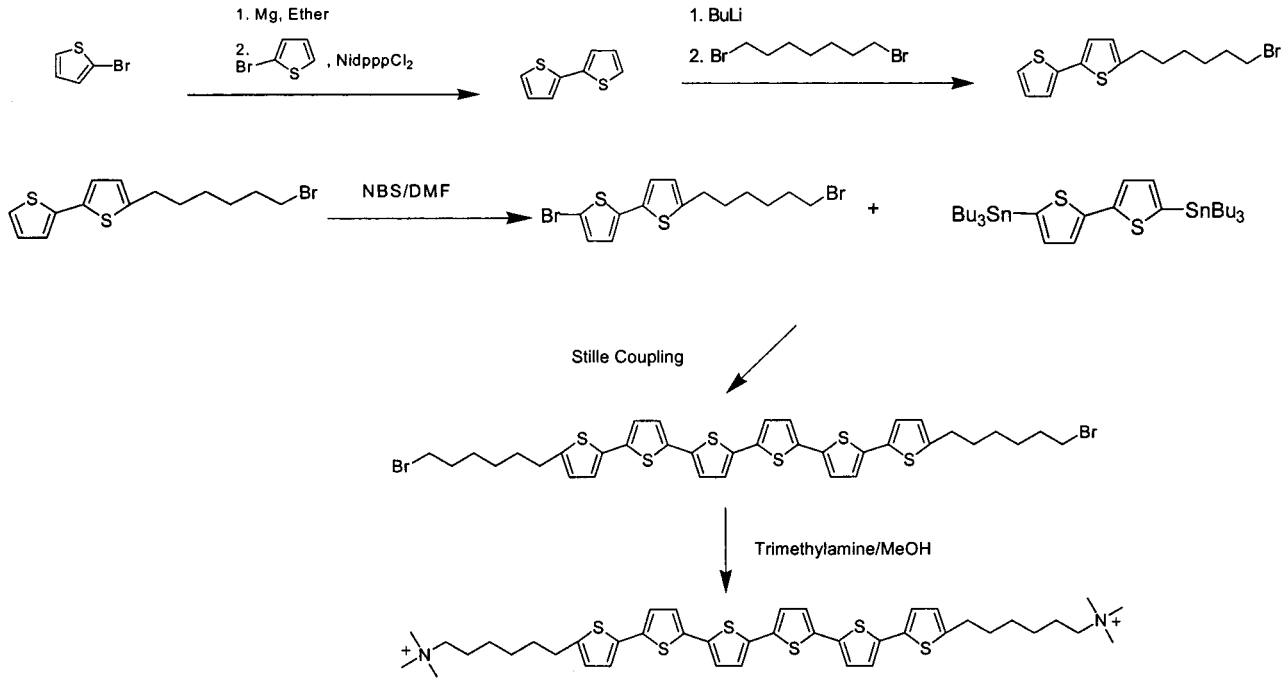

Figure 1. Synthesis scheme of sexithiophene (**6TN**).

mon method to fabricate organic transistors based on sexithiophene.[15] Recently, we have synthesized a bolaamphiphile with reasonable water solubility by introducing two pendant cationic alkyl end groups (trimethylamino-hexyl) at the α- and ω-positions of the sexithiophene molecule (structure shown in Figure 1).[16] We have shown that this bicationic molecule can be deposited from aqueous-based solutions to form well-ordered thin films with sodium polystyrene sulfonate (PSS), a polyanion, using alternating polyelectrolyte deposition.[17] This system has provided insight into the uniformity in film structural ordering of bolaform amphiphiles and oppositely charged polyelectrolytes, which have received intensive study over the past few years.[18]

A number of research groups have found interesting effects by introducing silicate clay with a conducting oligomer/polymer. Because of the unique layered structure of clay, anisotropic conductivity (perpendicular/parallel to the clay layer) was found in a polyphosphazene−montmorillonite composite polyelectrolyte material prepared by a bulk mixing process.[19] Several amino and nitro derivatives of bi-, ter-, and quarterthiophenes were intercalated into vermiculite clay by an ion exchange reaction and orientation of the confined oligothiophenes was studied.[20] Very recently, Eckel and Decher have fabricated OLEDs including an isolating montmonrillonite layer at different cycles of the layer-by-layer process.[21] They found that with the presence of a barrier layer, device performance increased by a factor of 14 or greater in comparison with that of the pure polymer system. They stated that the interfacial roughness plays an important role, although no data was made available.

In this work we investigate the role of clay layers in the preparation of nanostructured multilayer films of sexithiophene using the layer-by-layer approach for eventual FET applications. The hybrid ultrathin film is unique in that it incorporates inorganic insulating silicate layers and an organic semiconducting layer using the electrostatic layer-by-layer deposition technique. We believe that this is the first such system for the preparation of sexithiophene ultrathin films.[13,14] The goal is to find alternative methods to vacuum deposition for device preparation. Thus, alternating multilayer films of montmorillonite clay and bolaform sexithiophenes were prepared from pure aqueous and salt solution. A number of surface-sensitive spectroscopic and microscopic methods were used to characterize the films. Mostly, we emphasize the distinct structures and surface morphologies of samples prepared from two types of sexithiophene solutions: pure water and 0.1 M NaCl. The presence of salts affected the aggregation behavior and deposition of these films. The orientation of the sexithiophene and the long-range order observed plays an important role in determining future FET behavior.

Experimental Section

Materials. A bolaform amphiphile of quaternized-amine-terminated sexithiophene was synthesized using the scheme

(13) (a) Horowitz, G.; Fichou, D.; Peng, X.; Garnier, F. *Synth. Met.* **1991**, *41*−*43*, 1127. (b) Lovinger, A. J.; Rothberg, L. J. *J. Mater. Res.* **1996**, *11*, 1581.

(14) (a) Geiger, F.; Stoldt, M.; Schweizer, H.; Bauerle, P.; Umbach, E. *Adv. Mater.* **1993**, *5*, 922. (b) Horowitz, G.; Delannoy, P.; Bouchriha, H., et al. *Adv. Mater.* **1994**, *6*, 752.

(15) (a) Garnier, F.; Horowitz, G.; Peng, X.; Fichou, D. *Synth. Met.* **1991**, 45. (b) Garnier, F.; Yassar, A.; Hajlaoui, R.; Horowitz, G.; Deloffre, F.; Servet, B.; Ries, S.; Alnot, P. *J. Am. Chem. Soc.* **1993**, *115*, 8716.

(16) Xia, C.; Locklin, J.; Youk, J. H.; Advincula, R. C. *Langmuir* **2002**, *18*, 955.

(17) Locklin, J.; Youk, J. H.; Xia, C.; Park, M.-K.; Fan, X.; Advincula, R. C. *Langmuir* **2002**, *18*, 877.

(18) (a) Hong, J. -D.; Park, E.-S.; Park, A. L. *Langmuir* **1999**, *15*, 6515. (b) Saremi, F.; Tieke, B. *Adv. Mater.* **1998**, *5*, 388. (c) Mao, G.; Tsao, Y.-H.; Tirrell, M.; Davis, H. T. *Langmuir* **1994**, *10*, 4174.

(19) Hutchison, C. J.; Bissessur, R.; Shriver, F. D. *Chem. Mater.* **1996**, *8*, 1597.

(20) Ibrahim, M. A.; Lee B.-G.; Park, N.-G.; Rugh, J. R.; Eberl, D. D.; Frank, A. J. *Synth. Met.* **1999**, *105*, 35.

(21) Eckle, M.; Decher G. *Nano Lett.* **2001**, *1*, 45.

as shown in Figure 1. A more detailed description of the synthesis can be found elsewhere.[16] Two solutions of sexithiophene (abbreviated as **6TN**) were prepared in pure water and in 0.1 M NaCl. The **6TN** concentration of both systems was 1 wt %.

Montmorillonite Na^+ clay was provided by Southern Clay Product Corporation (Commercially Cloisite Nanoclay, CEC (cation exchange capacity) of 91−92 mequiv/100 g, density of 2.6 g/cm^3, noted as **MONT** hereafter). An aqueous dispersion was made by suspending 0.1 g of **MONT** powder in 1000 mL of deionized water (concentration 0.01 wt %). The yellowish dispersion was stirred with a blender at 2000 rpm overnight. Deionized water (resistivity = 18.2 MΩ cm, pH = 6.82) used in all experiments was purified by a Milli-Q Academic system (Millipore Corporation) with a 0.22-μm Millistack filter at the outlet. To achieve homogeneity of the aqueous systems, both **MONT** and **6TN** solutions were sonicated for half an hour right before each cycle of deposition.

Glass slides (Fisher Scientific, Inc.) were precleaned and pretreated before the layer-by-layer deposition processes.[22] Freshly peeled mica was used as the substrate to study the monolayer aggregation morphology deposited from **6TN** solutions. A boron-doped silicon wafer with a surface orientation of ⟨100⟩ (MEMC Electronic Materials, Inc.) was used as a substrate to investigate the monolayer clay particle morphology. All chemicals and reagents were purchased from Aldrich and used as-received. All organic solvents used were purified by distillation.

Multilayer Film Deposition on Glass Slides. The layer-by-layer deposition process consists mainly of the following steps:

1. Immerse the substrate into the solution of **6TN** for 30 min. Rinse the deposited substrate in deionized water and dry with air flow.

2. Immerse the substrate into the **MONT** dispersion for 15 min. Rinse the deposited substrate in deionized water and dry with air flow.

Repeating the above two-step process leads to the **6TN/MONT** hybrid multilayer formation, driven by electrostatic interaction at the interface boundaries. Samples of 1-layer to 20-layers were prepared manually.[23] Figure 2 schematically shows the composition and structure of the multilayer film. After deposition, all the samples were stored inside a desiccator in a clean room to avoid moisture and contamination.

Characterization. The UV−vis spectra of deposited glass slide samples were obtained using a Perkin-Elmer spectrometer (Lambda 20). X-ray diffraction analysis of clay powder and multilayer samples were done on a Phillips X'pert PW3040-MPD model diffractometer with Cu Kα (λ = 0.154 nm) as the incident beam. The basal distances were calculated from the peak positions using the Bragg equation. Atomic force microscopy (AFM) was used to investigate multilayer surface morphology. Micrographs were obtained using a PicoScan system (Molecular Imaging) equipped with an 8 × 8 μm scanner. A noncontact magnetic ac (MAC) mode was used for all the AFM images. A MAC lever, silicon nitride based cantilever coated with magnetic film, was used as the AFM tip. The force constant of the tip is 0.5 N/m and the resonance frequency is around 100 kHz. All samples were measured inside a suspension chamber to minimize ambient disturbance. The RMS (root mean square) roughness data of the sample surface was calculated using integrated software that came with the instrument.

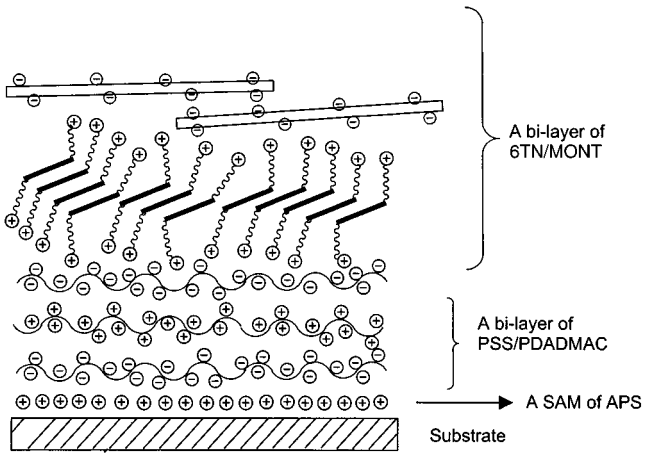

Figure 2. Schemetic representation of the **6TN/MONT** multilayer film.

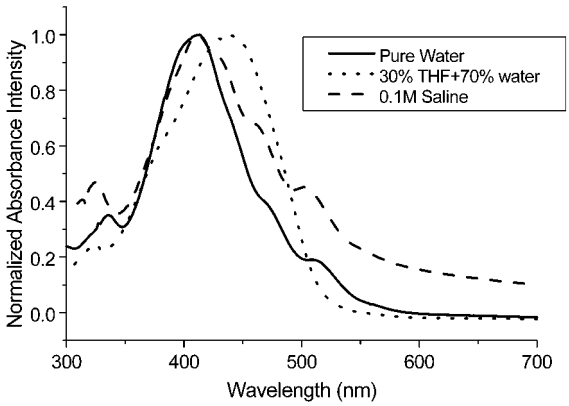

Figure 3. UV−vis absorbance spectra of the three types of **6TN** solutions.

Results and Discussion

UV−Vis Spectroscopy. As shown in Figure 1, the **6TN** molecule has a stiff hydrophobic sexithiophene unit and two short cationic alkyl arms at both ends. The two positively charged amine end groups render the molecule hydrophilic and water soluble. Although it is has reasonable solubility in water, it forms aggregates at relatively low concentrations because of the strong tendency toward $\pi-\pi$ stacking of the conjugated sexithiophene portion of the molecule.[16,17] Hence, this bolaform amphiphile shows unique aggregation behavior both in solutions and on surfaces. Fine structure of the oligothiophene aggregation has been observed and studied.[24]

The UV−vis absorption and aggregation property of **6TN** in solutions were first studied prior to its use for deposition. Figure 3 shows the spectra of **6TN** in three types of solutions. The strongest $\pi-\pi^*$ absorption peak occurs at about λ_{max} = 413 nm for both pure water and

(22) The substrates were first cleaned in a plasma cleaner under an Ar atmosphere for 350 s. They were then soaked in Piranha solution (3:7 (v/v) mixture of 30% (w/w) hydrogen peroxide and 98% (w/w) sulfuric acid) for 15 min and thoroughly rinsed by sonication in a deionized water bath. The purpose for the above precleaning process is to create a fresh hydroxylated surface suitable for the next step of SAM (self-assembled monolayer) formation. The precleaned substrates were submerged into freshly distilled toluene along with 0.5 wt % of APS (3-aminoproyltriethoxylsilane, Aldrich) for 30 min. The slides were then sonicated with toluene, acetone, and deionized water and stored in 0.1 M HCl overnight for protonation. Water contact angle measurements were taken before and after functionalization to ensure surface silanization by monitoring the change in hydrophilicity of the substrates. Two bilayers of oppositely charged PSS (poly sodium styrenesulfonate, MW ca. 70000, Aldrich)/PDADMAC (polydiallyldimethylammonium chloride, MW ca. 100000−200000, Aldrich) layers were introduced to provide an even charge distribution for **6TN** deposition.

(23) Here and after 1-layer refers to one **6TN**/**MONT** composite bilayer.

(24) (a) Fichou, D.; Horowitz, G.; Nishikitani, Y.; Garnier, F. *Synth. Met.* **1989**, *28*, C723. (b) Fichou, D.; Horowitz, G.; Xu, B.; Garnier, F. *Synth. Met.* **1992**, *48*, 167.

0.1 M saline systems. In both the pure water and 0.1 M NaCl systems, there are distinct "shoulders" brought about by a combination of the vibronic structure and/or Davydov interactions[25] of the aggregated sexithiophene molecules that can be seen at 430, 470, and 510 nm. These shoulders become more distinct and of a larger intensity with increasing salt concentration, indicating that there is more **6TN** molecular aggregation in solution upon the addition of salt. Also, the heightened spectral baseline confirms the larger aggregate size in the 0.1 M saline system since it leads to a greater light-scattering effect. To further study the aggregation behavior, 30% THF was introduced to the pure water system.[16] In this case, a significant red shift was seen from 413 to 438 nm and the lower energy shoulders disappear. These results indicate the disaggregation of the hydrophobic portion of **6TN** that occurs due to the increased solubility in THF. In other words, the H-aggregates ($\pi-\pi$ stacking) formed in water solution are dispersed, owing to a greater solvation brought about by the organic solvent.[26] This disaggregation of **6TN** can also explain the red shift of the absorbance peak of the 30% THF system, which is a lower energy absorption attributed to single molecules.

The UV−vis absorption and aggregation properties of **6TN** films were also recorded. Figure 4a,b shows the spectra of **6TN/MONT** multilayer samples prepared from pure water and 0.1 M NaCl. It should be noted that the absorbance intensity for the 0.1 M NaCl system increased by a factor of 5 as compared with that of pure water, which indicates much more **6TN** material was deposited between the **MONT** sheets from the saline solution. This result is further confirmed by XRD measurements. Similar to Figure 3, shoulders are found in a lower energy range, also indicating a larger amount of aggregation on the surface for 0.1 M NaCl. This aggregation augmentation also gives rise to the red shift of the λ_{max} when comparing the solution and film, which is 420 nm for a 0.1 M saline system and 445 nm for the pure water system. Similar to the solution aggregation properties discussed previously, the possible reason may be the former has more H-aggregation of **6TN** on the **MONT** surface. However, several interesting aspects should be pointed out as the absorbance curves of the pure water system in Figure 3 and Figure 4a are compared. First of all, a remarkably large red shift can be observed: $\lambda_{max} = 413$ nm in solution while $\lambda_{max} = 445$ nm on the surface. Also, the curve contour at a lower energy regime in Figure 4a is smoother than that in Figure 3. These results are due to a change in conformation and composition of the **6TN** aggregate between solution and upon adsorption at the surface. In other words, the interaction between the **6TN** molecules and the underlying clay sheets leads to a reordering of the aggregates on the surface. This is further clarified with the succeeding discussions.

From the two UV−vis spectra, the linear increase of absorbance intensity and area under each curve is typical for a stepwise and regular film thickness growth. The insets of parts a and b in Figure 4 show the relationship between peak intensity and number of

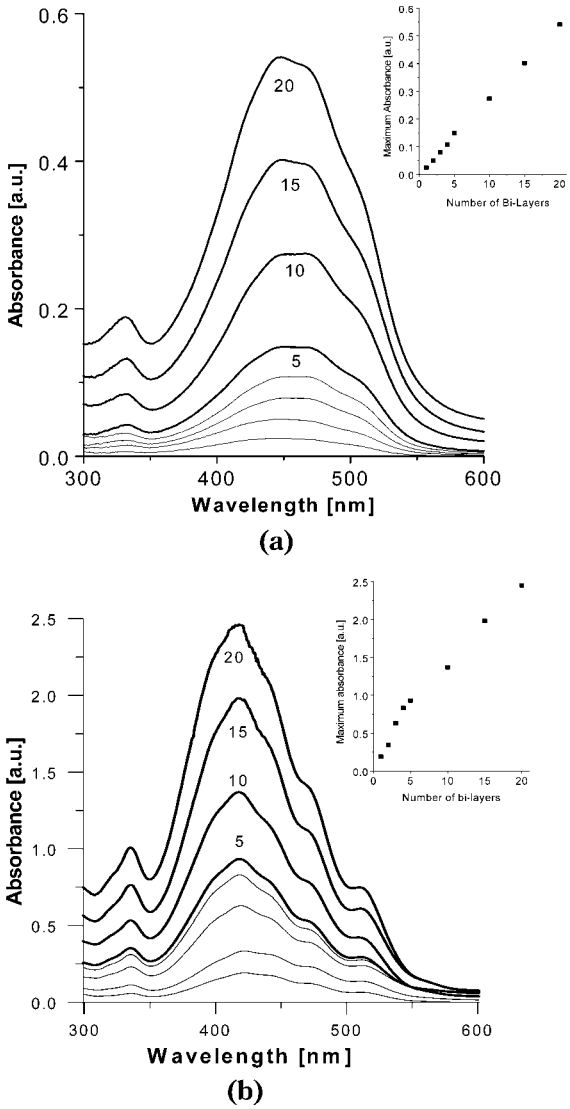

Figure 4. (a) UV−vis spectra of **6TN/MONT** multilayer films (1−20 layers) prepared from pure water. Peak absorbance versus number of bilayers is plotted in the inset. (b) UV−vis spectra of **6TN/MONT** multilayer films (1−20 layers) prepared from 0.1 M NaCl solution. Peak absorbance versus number of bilayers is plotted in the inset.

deposition cycles in the two systems. The linear increase provides evidence that the multilayer film of **6TN/MONT** possesses a uniform and well-ordered layer-by-layer structure, which is advantageous for future practical device fabrication quality. A similar linear thickness increase has been observed by ellipsometry and SPR (surface plasma resonance) for other clay/polyelectrolyte and polyelectrolyte/**6TN** combinations.[7,17] However, other studies of polyanion/polycation multilayer film from a saline system showed a linear to exponential thickness increase pattern when the salt concentration exceeded a "breakpoint" value.[27] A similar salt concentration effect is under further investigation with our **6TN/MONT** system.

X-ray Diffraction. With use of the Bragg equation, the *d*-spacing values (distance between the same side of two adjacent clay platelets) of untreated **MONT** powder samples and **6TN/MONT** multilayers were

(25) Muccini, M.; Lunedei, E.; Taliani, C.; Belijonne, D.; Cornil, J.; Bredas, J. L. *J. Chem. Phys.* **1998**, *109*, 10513.
(26) McRae, E.; Kasha, M. *J. Phys. Chem.* **1958**, *28*, 721.
(27) McAloney, R. A.; Sinyor, M.; Dudnik, V.; Goh, M. C. *Langmuir* **2001**, *17*, 6655.

calculated from XRD peak positions shown in Figure 5a−c. For pure clay, a (001) reflection occurs at $2\theta = 7.6°$, corresponding to a first-order *d* spacing of 1.16 nm, which was observed. Third- and fourth-order reflections were also observed at higher 2θ angles and the *d* spacings calculated as 1.33 and 1.26 nm, respectively. The data above gives an average *d*-spacing value of around 1.2 nm, which is very typical for pristine montmorillonite clay.[4]

Three multilayer samples from pure water system exhibited consistent XRD patterns as shown in Figure 5b. First- and fourth-order diffractions both give a defined *d*-spacing value of about 2 nm for this set of multilayer samples. The increase in *d*-spacing value clearly indicates the intercalation of **6TN** into the interlayer galleries of the clay platelets. Moreover, the *d* spacing also showed a significant increase when salt was added to the **6TN** solution. As shown in Figure 5c, an average *d*-spacing value of 3.5 nm was calculated from the first- and second-order diffractions for the three samples prepared from the 0.1 M saline system. Here, it is apparent that more **6TN** material was absorbed onto the **MONT** sheets in the case of the 0.1 M saline system. This result is consistent with the UV−vis measurements in terms of increased absorbance intensity. Similar studies have shown that the thickness of polyelectrolyte monolayer adsorbed on the surface can be drastically increased by the addition of electrolyte to the polymer solution.[18,28] The reason for this increased amount of absorber lies in the charge screening effect of additional counterions on the reduction of intra- and intermolecular electrostatic repulsion of the solute molecules.[29] Therefore, the **6TN** aggregate size in saline is larger than that in pure water. This result is consistent with the UV−vis solution measurement results shown in Figure 3. Thus, from the discussion above, it is easy to comprehend the fact that the *d* spacing of films prepared using the 0.1 M saline system is larger than that of the pure water system. Thus, both UV−vis and XRD measurements show more **6TN** material can be deposited from 0.1 M NaCl than from pure water. As a result, this greater amount of conducting oligomer deposited is expected to lead to better lateral conductivity of the multilayer film.[15] Again, this result is of practical significance for future microelectronic device preparation.

Furthermore, from the peak intensities shown in Figure 5b,c, as the number of layers increases, the diffraction intensities of the two sets of multilayer samples increases accordingly. This is because thicker film samples give larger diffraction volumes and hence higher diffraction peaks, indicating the gradual and steady buildup of the film thickness. Also, from the presence of higher order reflections and their increased intensities compared with those in an original clay powder XRD pattern, it is obvious that a well-defined and significant *z*-direction of layer-by-layer order is introduced to the **6TN/MONT** multilayer system. A similar XRD result was observed in our previous study on **PDADMAC/MONT** multilayer thin films.[30] Other results have also shown that the XRD pattern could not be due to just clay platelet aggregates, although it may

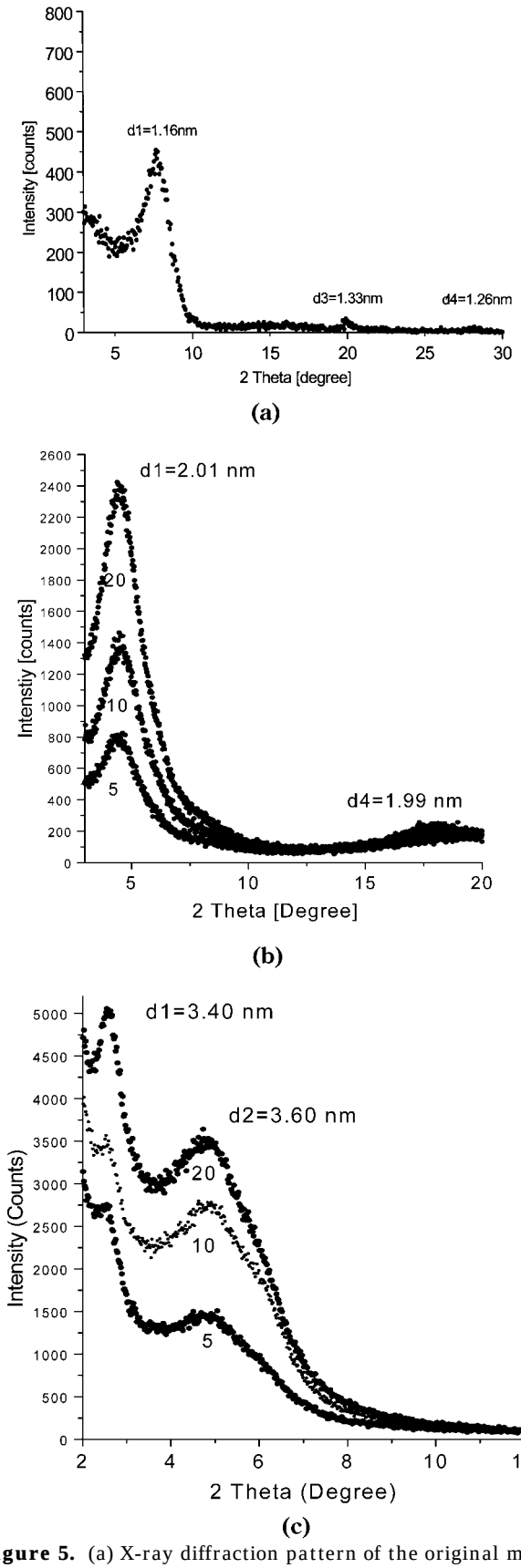

Figure 5. (a) X-ray diffraction pattern of the original montmorillonite clay sample. (b) X-ray diffraction patterns of multilayer films (5, 10, and 20 layers) deposited from pure water. (c) X-ray diffraction patterns of multilayer films (5, 10, and 20 layers) deposited from 0.1 M NaCl solution.

(28) (a) Hong, J.-D.; Kim, D. S.; Char, K. H.; Jin, J. I. *Synth. Met.* **1997**, *84*, 815. (b) Harmnond, T. P. *Macromolecules* **1997**, *30*, 7237.

(29) Decher, G.; Hong, J.-D.; Schmitt, J. *Thin Solid Films* **1992**, *210/211*, 831.

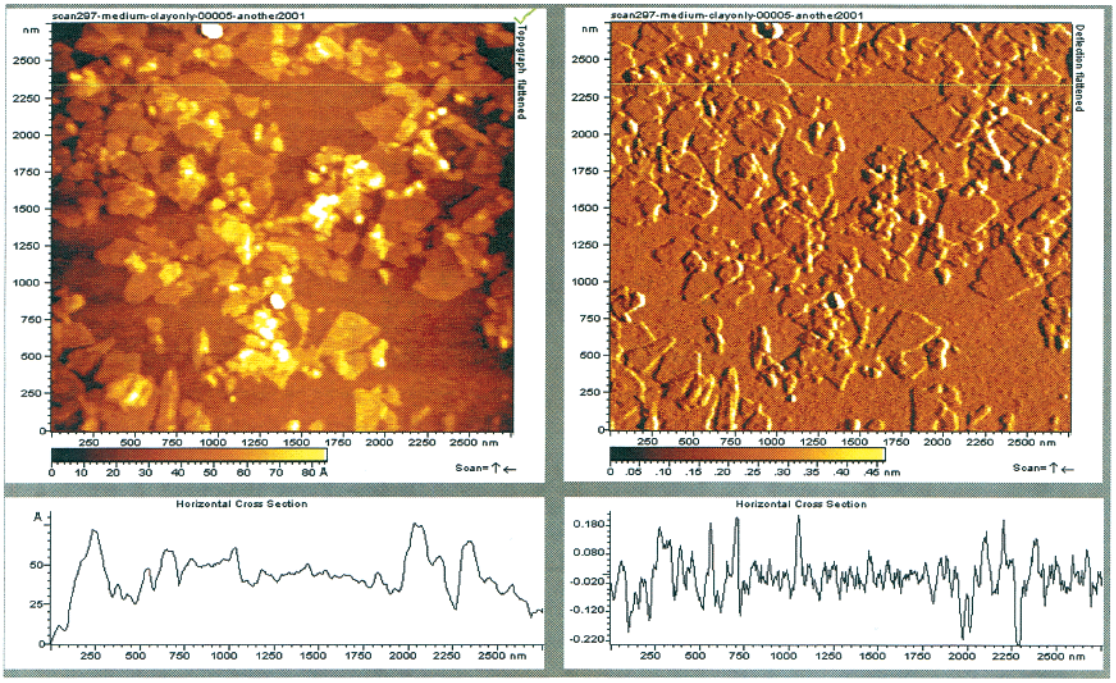

Figure 6. AFM morphology of montmorillonite particles: topographically flattened (left) and deflection flattened (right) image.

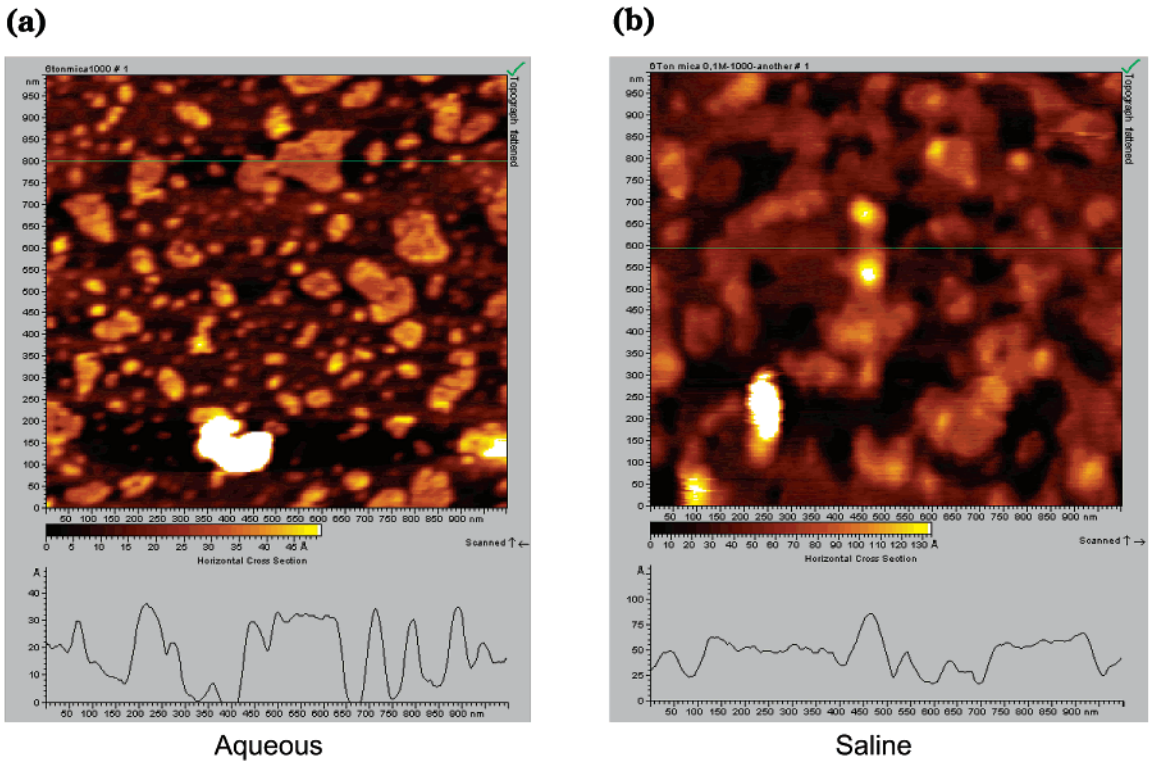

Figure 7. AFM morphology of **6TN** aggregates on mica (a) from pure water (left) and (b) from 0.1 M saline (right).

result in broadening of the Bragg peaks.[7,8,10] Thus, the UV−vis spectroscopy along with the XRD provides a consistent conclusion that well-ordered bolaform amphiphile/clay films can be easily obtained.

Atomic Force Microscopy. The morphology of **MONT** and **6TN** was first individually studied by AFM. Figure 6 shows the images of a single layer of untreated clay particles deposited from the **MONT** dispersion. The sample was prepared by placing a drop of dilute **MONT** solution on a piece of precleaned silicon wafer and evaporating the solvent. The platy shape and sharp edge profile of these particles is readily observed. Figure 6 also clearly demonstrates the approximate lateral size of these particles to be around a few hundred nanometers. Thus, the high aspect ratio property of these quasi-two-dimensional sheets is quite obvious since their thickness is just about 1 nm. Figure 7a,b shows the difference in **6TN** aggregate morphology between pure water and 0.1 M saline. The two samples were

(30) Fan, X.; Park, M.-K.; Xia, C.; Advincula, R. C. *J. Mater. Res.*, in press.

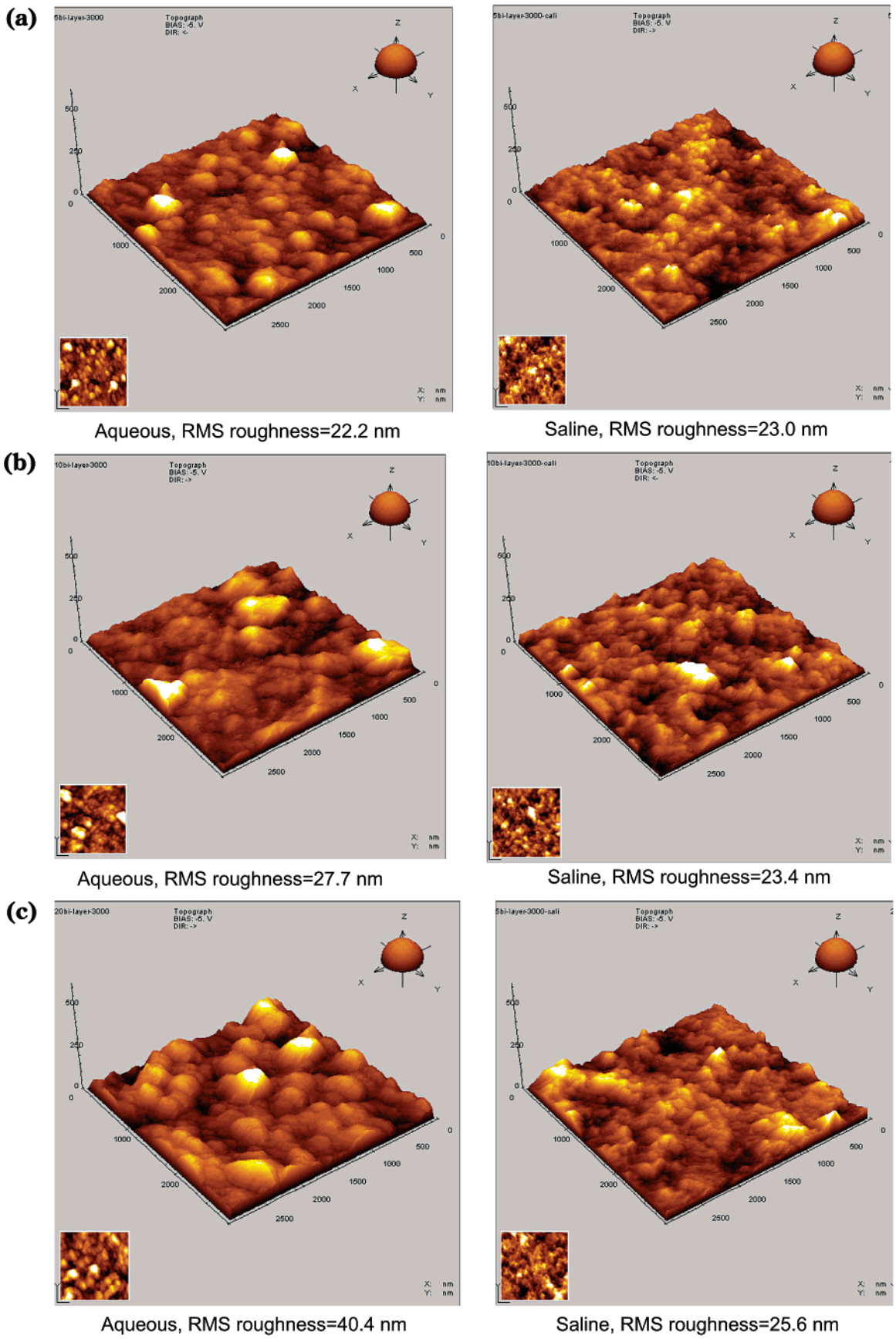

Figure 8. (a)−(c) Comparison of AFM images of multilayer samples with **6TN** on the surface prepared from two systems. (a) Comparison of 5-layer surface morphology and roughness. (b) Comparison of 10-layer surface morphology and roughness. (c) Comparison of 20-layer surface morphology and roughness.

prepared by immersing freshly peeled mica in two **6TN** solutions with the same deposition parameters as those of the multilayer samples. Since the mica surface is atomically flat and negatively charged upon hydration,

the **6TN** aggregation morphology can be rendered. First of all, the comparison in Figure 7 clearly shows that the saline system gives a larger *average* aggregate size. Also noticeably, the aggregate size from pure water is widely distributed, ranging from 100 to 200 nm to a few tens of nanometers, as can be seen from the line profile in Figure 7a. Moreover, these aggregates are separated from one another. As seen in Figure 7a, this discrete aggregation morphology leaves a significant part of the surface uncovered. In contrast, the aggregate size from saline systems is more evenly distributed. More interestingly and importantly, they form uniform and continuous **6TN** aggregate chains or domains on the surface. Thus, it is clear that the saline system provides more **6TN** surface coverage, which is consistent with UV−vis absorption intensity and XRD *d*-spacing data.

Noticeably in Figure 7a, it is obvious that the smaller (lateral size below 50 nm) aggregates greatly outnumber larger aggregates (lateral size above 50 nm). This observation is consistent with our speculation from UV−vis data. A comparison of the reorientation of the molecules may occur when **6T** aggregates adsorb onto the clay surface, which is driven by a minimization of energy. However, the mechanism behind this phenomenon is yet unknown.

Surface morphology and roughness change of multilayer samples was monitored by AFM with **6TN** as the outer layer. Figure 8a−c demonstrates a series of surface morphologies of 5-, 10-, and 20-layer samples. From previous discussions, since the **6TN** aggregates from the saline system form a more continuous pattern and complete coverage, the RMS roughness of this set does not increase dramatically when moving from 5 to 20 layers (23.0, 23.4, and 25.6 nm for three samples). We have found similar roughness results in other systems such as **PDADMAC/MONT** multilayers prepared using the layer-by-layer technique.[28] The smoothness of the surface is believed to be related to the unique property of a high aspect ratio of the clay particle: the two-dimensional sheets can cover the defects of the underlying layer. Kleinfeld and Ferguson also drew a conclusion that the linear thickness increase indicates the clay/**PDADMAC** multilayer system is "self-healing".[5] In contrast with most alternate polyeletrolyte deposition (APD) systems that mainly involve oppositely charged polymer, incorporating clay into the system has great significance in terms of surface smoothness since the former is less capable of recovering the disorder found underneath.[31] Thus, it is not hard to imagine that the next layer of **MONT** sheets readily roofs the smaller empty spaces and this smoothening effect leads to a relatively flat substrate for the next layer of **6TN**. In other words, the surface smoothness is reproduced possibly by **MONT** coverage in the case of the **6TN/MONT** multilayer prepared from 0.1 M NaCl.

However, from the surface characteristic of the samples in the pure aqueous system, it can be seen that the larger **6TN** aggregates gradually dominate the surface features while smaller aggregates become overshadowed and less visible in the spaces among the bigger ones. As a result, the surface turns rougher as the thickness increases. The RMS roughness data increased from 22.2 to 27.7 to 40.4 nm for the three multilayer samples. In other words, the rougher subsequent layer reflects the roughness from the previous layers. The reason for this dramatic roughness increase is probably because the clay sheets are unable to cover the sublayer defects since the bigger **6TN** aggregate size is on a comparable scale to the clay particle lateral dimensions. Moreover, isolated and unevenly distributed aggregates make it harder for the subsequent layer of **MONT** plates to cover the bigger empty space among them, leaving "holes and trenches" on the surface. The roughness resulting from these defects can be further aggravated as another layer of isolated and unevenly distributed aggregates are deposited, giving increased roughness for this series of samples prepared from a pure water system.

From the discussion above, the **6TN/ MONT** multilayers prepared from the saline system reveal better surface smoothness and ordering than those from a pure aqueous solution. These results are of considerable importance for future device fabrication. Further investigation is underway with regards to the salt concentration effect on solution and surface aggregation properties and thin film structure and morphology. This is primarily for optimizing surface coverage and smoothness. We are collaborating with other groups on the evaluation of the transistor activity of the films.

Conclusions

We have compared the structure and morphology of **6TN/MONT** multilayer thin films prepared from pure water and 0.1 M NaCl systems. The **6TN** amphiphile showed unique aggregation behavior both in solution and on the surface. In aqueous solution, the aggregate size became larger upon the addition of salt and disaggregation occurred with the addition of 30% THF. On clay surfaces, the aggregates deposited from 0.1 M saline have a more uniform size distribution and surface coverage than that from a pure water system. UV−vis spectra showed much higher absorbance intensity of the samples prepared from 0.1 M saline. XRD *d*-spacing data showed 2 nm for the pure water system and 3.5 nm for 0.1 M saline, indicating a thicker **6TN** layer deposited from the latter. Better **6TN** surface smoothness from 0.1 M saline was observed by AFM. The idea of incorporating more **6TN** species absorbed on the surface while yielding a smoother surface morphology have great significance and could lead to better device quality.

Acknowledgment. We thank Dr. Yogesh Vohra and Dr. Shane Catledge in the physics department of the University of Alabama at Birmingham for their help on XRD measurements and Southern Clay Product Incorporation for the clay samples. Technical support from Molecular Imaging and Optrel GbR is acknowledged. Financial support from NSF, CAREER -DMR (99-82010), Army Research Office (DAAD-19-99-1-0106), Alabama tri-campus materials science program (Xiaowu Fan), Alabama Project SEED (Wally Blanton), and the GAANN fellowship (Jason Locklin) are greatly acknowledged.

CM011519C

(31) Tillman, N.; Ulman, A.; Penner, L. T. *Langmuir* **1989**, *5*, 101.